

Understanding the different rotational behaviors of ^{252}No and ^{254}No

H. L. Liu,^{1,*} F. R. Xu,² and P. M. Walker^{3,4}

¹*Department of Applied Physics, Xi'an Jiaotong University, Xi'an 710049, China*

²*School of Physics, Peking University, Beijing 100871, China*

³*Department of Physics, University of Surrey, Guildford, Surrey GU2 7XH, UK*

⁴*CERN, CH-1211 Geneva 23, Switzerland*

Total Routhian surface calculations have been performed to investigate rapidly rotating transfermium nuclei, the heaviest nuclei accessible by detailed spectroscopy experiments. The observed fast alignment in ^{252}No and slow alignment in ^{254}No are well reproduced by the calculations incorporating high-order deformations. The different rotational behaviors of ^{252}No and ^{254}No can be understood for the first time in terms of β_6 deformation that decreases the energies of the $\nu j_{15/2}$ intruder orbitals below the $N = 152$ gap. Our investigations reveal the importance of high-order deformation in describing not only the multi-quasiparticle states but also the rotational spectra, both providing probes of the single-particle structure concerning the expected doubly-magic superheavy nuclei.

PACS numbers: 21.10.Re, 21.60.Cs, 23.20.Lv, 27.90.+b

Together with the exploration of nuclei far away from the stability line using radioactive nuclear beams, the synthesis of superheavy nuclei towards the predicted “island of stability” by fusion reactions is the focus of current research on atomic nuclei [1, 2]. The occurrence of superheavy nuclei owes to the quantum shell effect (see, e.g., Ref. [3]) that overcomes the strong Coulomb repulsion between the large number of protons. The shell effect peaks at the expected doubly-magic nucleus next after ^{208}Pb , the center of the stability island. Unfortunately, various theories give rise to different magic numbers and available experiments have not been able to confirm or exclude any of them. Nevertheless, one can obtain single-particle information that is intimately related to the shell structure of superheavy nuclei from transfermium nuclei where γ -ray spectroscopy has been accessible for experiments [4, 5].

Transfermium nuclei have been found to be deformed. For example, $\beta_2 \approx 0.27$ has been derived for ^{254}No from the measured ground-state band [6]. The observation of K isomers with highly-hindered decays in ^{254}No [7–9] points to an axially-symmetric shape for the nucleus. The deformation can bring the single-particle levels from the next shell across the predicted closure level to the Fermi surface. They play an active role in both nuclear non-collective and collective motions that in turn can serve as probes of the single-particle structure. For example, the observed $K^\pi = 3^+$ state formed by broken-pair excitation in ^{254}No is of special interest [7]. This is because the $\pi 1/2^-$ [521] orbital occupied by one unpaired nucleon stems from the spherical orbital $2f_{5/2}$ whose position relative to the spin-orbit partner $2f_{7/2}$ determines whether $Z = 114$ is a magic number for the “island of stability”. On the other hand, high- j intruder orbitals sensitively respond to the Coriolis force during collective

rotation. The observation of upbending or backbending phenomena is usually associated with the alignment of high- j intruder orbitals. The spectroscopy experiments on transfermium nuclei provide a testing ground for the theoretical models that are used to predict the properties of superheavy nuclei.

Modern in-beam spectroscopy experiments have observed rotational bands up to high spins, such as in the even-even nuclei ^{246}Fm [10], ^{248}Fm [4], ^{250}Fm [11, 12], ^{252}No [13], and ^{254}No [6, 14]. Especially, the yrast spectrum of ^{254}No has been extended to spins of more than $20\hbar$ because of the relatively high production rate. Theoretically, various models have been applied to study the rotational properties of transfermium nuclei. The calculations include: (i) cranking approximations of mean-field models such as the macroscopic-microscopic approach [15–17], the Nilsson potential with the particle-number-conserving method [18–20], the Hartree-Fock-Bogoliubov (HFB) approach with the Skyrme force [21, 22], the HFB approach with the Gogny force [23, 24], and the relativistic Hartree-Bogoliubov approach [25]; (ii) the projected shell model [26–28] that incorporates beyond-mean-field effects, restored symmetry and configuration

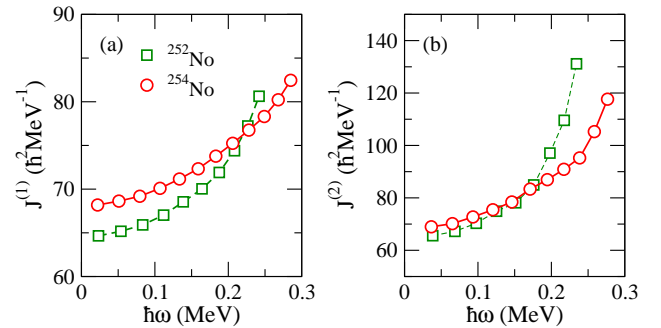


FIG. 1: (Color online) Experimental kinematic (a) and dynamic (b) moments of inertia for $^{252,254}\text{No}$. Data are taken from Refs. [13] and [14] for ^{252}No and ^{254}No , respectively.

*Electronic address: hlliu@mail.xjtu.edu.cn

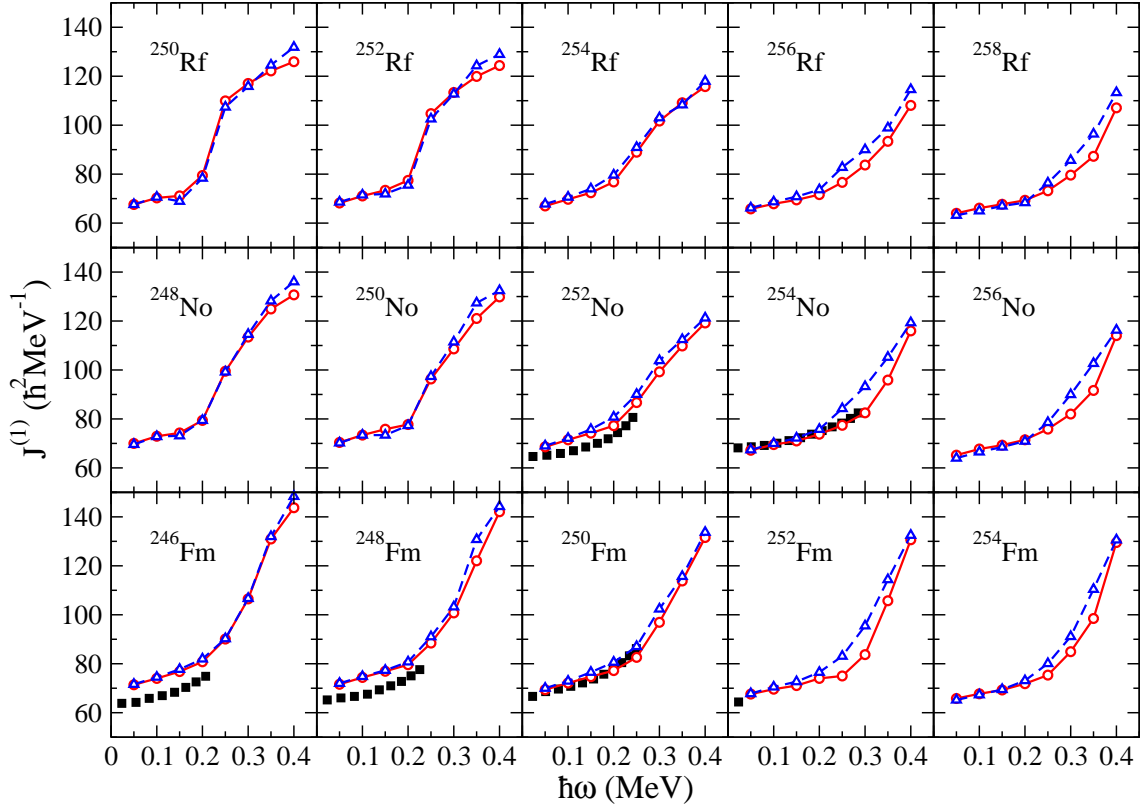


FIG. 2: (Color online) Calculated kinematic moments of inertia for Fm, No, and Rf isotopes, compared with available experimental data [4–6, 10–14]. Calculations with and without high-order deformations $\beta_{6,8}$ are represented by open circles (red) and open triangles (blue), respectively. Filled squares (black) indicate experimental data.

mixing. In general, the theories can reproduce the observations.

However, it is still an open question why ^{252}No and ^{254}No exhibit significantly different rotational behavior at high spins. The difference has been noticed since 2001 when the rotational band up to $I = 20$ in ^{252}No was first observed [13]. In Fig. 1, the experimental moments of inertia (MOIs) are displayed for $^{252,254}\text{No}$. It is seen that the MOIs of both nuclei increase gradually with rotational frequency at low spins. When reaching $\hbar\omega \approx 0.2$ MeV, the ^{252}No MOI grows sharply, while the ^{254}No MOI remains steady until a rotational frequency approaching 0.3 MeV. Although the previous various calculations can reproduce the MOIs of ^{252}No and ^{254}No , no one has explained in detail the mechanism responsible for the significant MOI difference of the two nuclei. Using total Routhian surface (TRS) calculations, now extended to include high-order deformations, we show that the difference can be understood in terms of β_6 that decreases the energies of the $\nu j_{15/2}$ intruder orbitals below the $N = 152$ deformed shell gap. We note that Schunck *et al.* [29] performed TRS calculations with high-order deformations. However, they did not include pairing correlations, which are necessary for the description of upbending and backbending phenomena.

The TRS approach [30–32] adopted here is a pairing-

deformation-frequency self-consistent calculation based on the cranked shell model. The single-particle states are obtained from the axially deformed Woods-Saxon potential [33] with the parameter set widely used for cranking calculations. Both monopole and doubly-stretched quadrupole pairings are included. The monopole pairing strength (G) is determined by the average-gap method [34], and the quadrupole pairing strengths are obtained by restoring the Galilean invariance broken by the seniority pairing force [35]. The quadrupole pairing has negligible effect on energies, but it is important for the proper description of MOIs [31]. An approximate particle-number projection is carried out by means of the Lipkin-Nogami method [36], thus avoiding the spurious collapse of pairing correlations at high angular momentum. For any given deformation and rotational frequency, the pairings are self-consistently calculated by the HFB-like method [30], so the dependence of pairing correlations on deformation and frequency is properly treated. The total energy of a state consists of a macroscopic part that is obtained with the standard liquid-drop model [37], a microscopic part that is calculated by the Strutinsky shell-correction approach [38], and the contribution due to rotation. At each frequency, the deformation of a state is determined by minimizing the TRS calculated in a multi-dimensional deformation space.

In the present work, the deformation space includes β_2 , β_4 , β_6 , and β_8 degrees of freedom. Transfermium nuclei around ^{254}No have been predicted to have β_6 deformations [16, 17]. It has been demonstrated that the β_6 deformation leads to enhanced deformed shell gaps at $Z = 100$ and $N = 152$ [39], and has remarkable influence on the binding energy [40], ground-state MOI [16], and K -isomer excitation energy [41]. With the inclusion of $\beta_{6,8}$ deformations in the TRS calculation, we investigate their effect on the collective rotation at high spins.

Figure 2 displays the kinematic MOIs calculated with and without high-order deformations for Fm, No, and Rf isotopes. All the calculations are performed without any adjustment of the parameters. When compared with experiments, the calculations including $\beta_{6,8}$ deformations are in good agreement with the data for ^{250}Fm and ^{254}No . In particular, we reproduce well the slow alignment observed in ^{254}No . Here an upbending is predicted beyond $\hbar\omega \approx 0.3$ MeV. The upbending at $\hbar\omega \approx 0.2$ MeV observed in ^{250}Fm is also reproduced well. Our calculations, however, overestimate the measured MOIs in $^{246,248}\text{Fm}$ and ^{252}No . Nevertheless, the theoretical variation trends are consistent with observations. It is worth noting that the observed quick growth of MOI at $\hbar\omega \approx 0.2$ MeV in ^{252}No is also shown in our calculation. For $^{246,248}\text{Fm}$, we predict the occurrence of upbending at $\hbar\omega \approx 0.2$ MeV that is in the proximity of the available experimental values. A few more data points will test the predictions.

Similar overestimation of the MOI in TRS calculations has also been seen in rare-earth nuclei, which is ascribed to the deficiency of the monopole pairing strength given by the average gap method [42]. It was found that an improved pairing strength can be obtained by matching the experimental and theoretical odd-even mass differences. The new pairing strength, including mean-field and blocking effects, results in a better description of the MOI [42] and the multi-quasiparticle state excitation energy [43]. Nevertheless, the adjustment of G seems to barely affect the backbending/upbending frequency. Since the variation trends of the observed MOIs in transfermium nuclei can be reproduced and the present focus is on the high-spin property difference between ^{252}No and ^{254}No , we do not fine tune the pairing strength in this work.

The backbending/upbending phenomenon in the MOI is usually associated with the rotation alignment of high- j intruder orbitals near the Fermi surface. In the transfermium region, the intruder orbitals are $\pi i_{13/2}$ for protons and $\nu j_{15/2}$ for neutrons. The relativistic Hartree Bogliubov model [25], the cranked shell model with particle number conservation [20], and the projected shell model [28] all indicated the competitive alignments of $\pi i_{13/2}$ and $\nu j_{15/2}$ orbitals that take place simultaneously. Our calculations show, however, that the upbending is mostly ascribed to the alignment of the $\nu j_{15/2}$ orbital, with some contribution from the $\pi i_{13/2}$ orbital. This can be seen in Fig. 3 where the calculated neutron MOI of ^{252}No suddenly increases at $\hbar\omega \approx 0.2$ MeV, while the

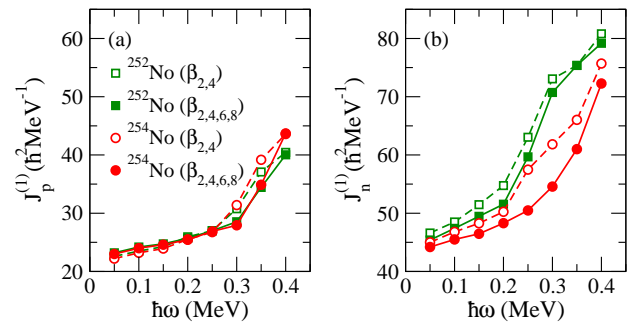


FIG. 3: (Color online) Proton (a) and neutron (b) components of the calculated kinematic moments of inertia for $^{252,254}\text{No}$.

proton component upbends later and contributes less angular momentum.

The upbending behavior changes with particle numbers. It can be seen in Fig. 2 that the increase of MOI becomes less drastic with increasing neutron and proton numbers. This is because the Fermi surface moves to be near the higher- Ω (single-particle angular momentum projection on the symmetry axis) branches of the $\pi i_{13/2}$ and $\nu j_{15/2}$ orbitals. Such branches tend to be deformation aligned, so that the nucleus gains collective angular momentum more slowly.

Figure 2 also presents the comparison between the MOIs calculated with and without high-order deformations. It shows that both calculations generate almost the same MOIs for $N < 152$ nuclei. However, the $N \geq 152$ nuclei have smaller MOIs at $\hbar\omega \approx 0.25 - 0.35$ MeV and hence slower alignments in the calculations with $\beta_{6,8}$, than in the calculations without $\beta_{6,8}$. The effect comes from β_6 deformation, while the influence of β_8 deformation is negligible.

^{254}No is, among others, the nucleus influenced the most by β_6 deformation. The calculation restricted to include only $\beta_{2,4}$ gives rise to an upbending at $\hbar\omega \approx 0.2$ MeV. This is in contrast to the gradual increase of MOI until $\hbar\omega \approx 0.3$ MeV in the calculation incorporating high-order deformations, which is what is observed in experiments. Much different from ^{254}No , ^{252}No has a MOI barely affected by β_6 deformation, with an upbending observed and also calculated to occur at $\hbar\omega \approx 0.2$ MeV. A similar difference is shown between ^{250}Fm and ^{252}Fm in our calculations (see Fig. 2). Here the difference is even more distinct. ^{250}Fm has a more drastic alignment than ^{252}No , and ^{252}Fm shows a more gentle alignment than ^{254}No . The two isotopes would have basically the same alignment behaviors if the β_6 deformation is ignored. The prediction in $^{250,252}\text{Fm}$ awaits experimental confirmation. The former already has data available around the upbending frequency, but the latter is poorly known in spectroscopy measurements besides the 2_1^+ state.

It has been demonstrated that β_6 deformation leads to enhanced deformed shell gaps at $Z = 100$ and $N = 152$ [39, 41]. The enlargement of the deformed shell gaps

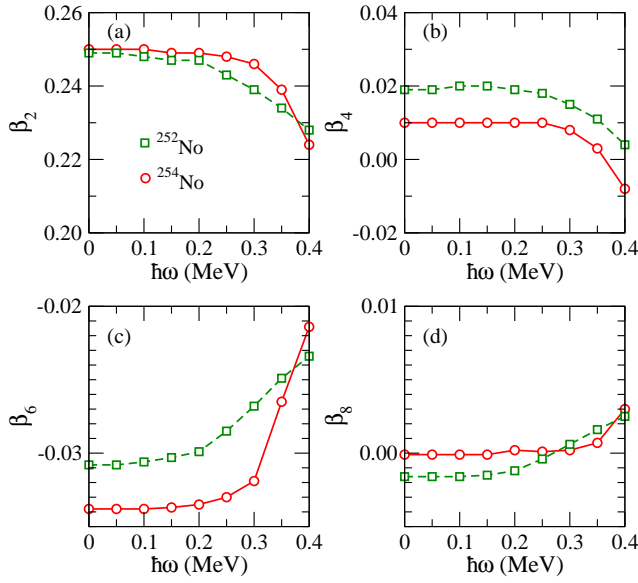


FIG. 4: (Color online) Calculated β_2 (a), β_4 (b), β_6 (c), and β_8 (d) deformations versus rotational frequency for $^{252,254}\text{No}$.

is accompanied by a lowering in energy of the $\pi i_{13/2}$ and $\nu j_{15/2}$ orbitals below the gaps. It is likely that the shift of the high- j intruder orbitals by β_6 deformation results in the slow alignment of ^{254}No . In Fig. 3, we display the proton and neutron components of the calculated MOIs for $^{252,254}\text{No}$. The comparison indicates that the slow alignment of ^{254}No mainly originates from the influence of β_6 deformation on the neutron MOI. This is because the shell gap at $N = 152$ is more enhanced than at $Z = 100$ and the neutron intruder orbital has a higher j value

than the proton one.

The deformations of $^{252,254}\text{No}$ are calculated to change with increasing rotational frequency, as shown in Fig. 4. The deformation changes are intimately related to the rotation alignments of the $\pi i_{13/2}$ and $\nu j_{15/2}$ orbitals. For ^{254}No , the $\beta_{2,4,6,8}$ deformations all keep almost constant at first and then sharply change at $\hbar\omega \approx 0.3$ MeV. In contrast, the large changes for ^{252}No take place at $\hbar\omega \approx 0.2$ MeV.

In summary, TRS calculations extended to include $\beta_{6,8}$ deformations have been performed to investigate collective rotations in transfermium nuclei. The calculated MOIs agree satisfactorily with available data. In particular, our calculations reproduce well the slow alignment observed in ^{254}No and the fast alignment observed in ^{252}No . The underlying mechanism responsible for the difference between ^{252}No and ^{254}No is found for the first time to lie in β_6 deformation that lowers the energies of the $\nu j_{15/2}$ intruder orbitals below the $N = 152$ gap. A more distinct difference is predicted for the $^{250,252}\text{Fm}$ isotopes. Our calculations indicate that β_6 deformation plays a vital role around $N = 152$ and $Z = 100$. The inclusion of β_6 deformation results in more realistic single-particle levels and hence has remarkable influence on not only the multi-quasiparticle states [41] but also the rotational spectra. The present work establishes a consistent relation between high-order deformations, MOIs and excitation energies of multi-quasiparticle states.

This work was supported by the Scientific Research Supporting Plan of Xi'an Jiaotong University under Grant No. 08142021; the National Natural Science Foundation of China under Grant No. 10975006; and the UK STFC and AWE plc.

-
- [1] S. Hofmann and G. M nzenberg, Rev. Mod. Phys. **72**, 733 (2000).
 - [2] Yu. Oganessian, J. Phys. G **34**, R165 (2007).
 - [3] M. Bender, W. Nazarewicz, P.-G. Reinhard, Phys. Lett. B **515**, 42 (2001).
 - [4] R.-D. Herzberg and P. T. Greenlees, Prog. Part. Nucl. Phys. **61**, 674 (2008).
 - [5] R.-D. Herzberg and D. M. Cox, Radiochim. Acta **99**, 441 (2011).
 - [6] P. Reiter *et al.*, Phys. Rev. Lett. **82**, 509 (1999).
 - [7] R.-D. Herzberg *et al.*, Nature (London) **442**, 896 (2006).
 - [8] S. K. Tandel *et al.*, Phys. Rev. Lett. **97**, 082502 (2006).
 - [9] R. M. Clark *et al.*, Phys. Lett. B **690**, 19 (2010).
 - [10] J. Piot *et al.*, Phys. Rev. C **85**, 041301(R) (2012).
 - [11] J. E. Bastin *et al.*, Phys. Rev. C **73**, 024308 (2006).
 - [12] P. T. Greenlees *et al.*, Phys. Rev. C **78**, 021303(R) (2008).
 - [13] R.-D. Herzberg *et al.*, Phys. Rev. C **65**, 014303 (2001).
 - [14] S. Eeckhaudt *et al.*, Eur. Phys. J. A **26**, 227 (2005).
 - [15] I. Muntian, Z. Patyk, and A. Sobiczewski, Phys. Rev. C **60**, 041302(R) (1999).
 - [16] I. Muntian, Z. Patyk, and A. Sobiczewski, Phys. Lett. B **500**, 241 (2001).
 - [17] A. Sobiczewski, I. Muntian, and Z. Patyk, Phys. Rev. C **63**, 034306 (2001).
 - [18] X.-T. He, Z.-Z. Ren, S.-X. Liu, and E.-G. Zhao, Nucl. Phys. A **817**, 45 (2009).
 - [19] Z.-H. Zhang, J.-Y. Zeng, E.-G. Zhao, and S.-G. Zhou, Phys. Rev. C **83**, 011304(R) (2011).
 - [20] Z.-H. Zhang, X.-T. He, J.-Y. Zeng, E.-G. Zhao, and S.-G. Zhou, Phys. Rev. C **85**, 014324 (2012).
 - [21] T. Duguet, P. Bonche, P.-H. Heenen, Nucl. Phys. A **679**, 427 (2001).
 - [22] M. Bender, P. Bonche, T. Duguet, and P.-H. Heenen, Nucl. Phys. A **723**, 354 (2003).
 - [23] J. L. Egido and L. M. Robledo, Phys. Rev. Lett. **85**, 1198 (2000).
 - [24] J.-P. Delaroche, M. Girod, H. Goutte, J. Libert, Nucl. Phys. A **771**, 103 (2006).
 - [25] A. V. Afanasjev, T. L. Khoo, S. Frauendorf, G. A. Lalazissis, and I. Ahmad, Phys. Rev. C **67**, 024309 (2003).
 - [26] Y. Sun, G.-L. Long, F. Al-Khudair, and J. A. Sheikh, Phys. Rev. C **77**, 044307 (2008).
 - [27] Y.-S. Chen, Y. Sun, and Z.-C. Gao, Phys. Rev. C **77**, 061305(R) (2008).

- [28] F. Al-Khudair, G.-L. Long, and Y. Sun, Phys. Rev. C **79**, 034320 (2009).
- [29] N. Schunck, J. Dudek, and B. Herskind, Phys. Rev. C **75**, 054304 (2007).
- [30] W. Satuła, R. Wyss, and P. Magierski, Nucl. Phys. A **578**, 45 (1994).
- [31] W. Satuła and R. Wyss, Phys. Scr. **T56**, 159 (1995).
- [32] F. R. Xu, W. Satuła, and R. Wyss, Nucl. Phys. A **669**, 119 (2000).
- [33] S. Ćwiok, J. Dudek, W. Nazarewicz, S. Skalski, and T. Werner, Comput. Phys. Commun. **46**, 379 (1987).
- [34] P. Möller and J. R. Nix, Nucl. Phys. A **536**, 20 (1992).
- [35] H. Sakamoto and T. Kishimoto, Phys. Lett. B **245**, 321 (1990).
- [36] H. C. Pradhan, Y. Nogami, and J. Law, Nucl. Phys. A **201**, 357 (1973).
- [37] W. D. Myers and W. J. Swiatecki, Nucl. Phys. **81**, 1 (1966).
- [38] V. M. Strutinsky, Nucl. Phys. A **95**, 420 (1967).
- [39] Z. Patyk and A. Sobiczewski, Phys. Lett. B **256**, 307 (1991).
- [40] Z. Patyk and A. Sobiczewski, Nucl. Phys. A **533**, 132 (1991).
- [41] H. L. Liu, F. R. Xu, P. M. Walker, and C. A. Bertulani, Phys. Rev. C **83**, 011303(R) (2011).
- [42] F. R. Xu, R. Wyss, and P. M. Walker, Phys. Rev. C **60**, 051301(R) (1999).
- [43] F. R. Xu, P. M. Walker, J. A. Sheikh, and R. Wyss, Phys. Lett. B **435**, 257 (1998).